Available online at www.sciencedirect.com

ScienceDirect

Ceramics International 40 (2014) 3953–3959

CERAMICS INTERNATIONAL

www.elsevier.com/locate/ceramint

# Quality improvement of single crystal 4H SiC grown with a purified β-SiC powder source

Jun Gyu Kim[a], Eun Jin Jung[a,b], Younghee Kim[b], Yuri Makarov[c], Doo Jin Choi[a,*]

[a]Department of Materials Science and Engineering, Yonsei University, 134 Shinchon-dong, Sudaemun-ku, Seoul 120-749, Republic of Korea
[b]Korea Institute of Ceramic Engineering and Technology, 233-5 Gasan-dong, Guemcheon-gu, Seoul 153-801, Republic of Korea
[c]Nitride Crystal Inc., 10404 Patterson Avenue, Suite 108, Richmond, VA 23238, USA

Received 15 July 2013; received in revised form 16 July 2013; accepted 8 August 2013
Available online 16 August 2013

**Abstract**

In the processing of single crystal SiC using the PVT method, defects such as micropipes and dislocations occur due to various reasons, including growth rate, temperature gradient, seed quality, pressure change and the SiC source powder. Among these factors, the SiC source powder was investigated to reduce defects in single crystal SiC. β-SiC powder was used to reduce the growth temperature and change basic properties of the particle, including microstructure, particle size and chemical composition, through the purification process. The structure of the purified β-SiC particle was changed into a spherical structure and its particle size expanded. Chemical analysis revealed reduced free carbon, oxide phases such as silica ($SiO_2$), silicon oxycarbide and metallic impurities. Purified β-SiC powder showed increased particle size of 37 μm and showed improved purity. With this, we grew single crystal 4H SiC and compared the micropipe and dislocation density to that of single crystal 4H SiC grown with non-purified β-SiC powder. The experimental results confirmed that the 4H SiC wafer grown by purified β-SiC powder exhibited improved quality.


*Keywords:* Purified β-SiC powder; Chemical composition; Single crystal 4H SiC; Micropipe and dislocation density

## 1. Introduction

Silicon carbide (SiC) is used in many areas as it has outstanding mechanical properties, including high elastic modulus and hardness, excellent thermal and electrical properties such as high thermal conductivity and a wide bandgap, and stable chemical properties. While SiC can have 200 or more polytypes, the α-type phase (4H and 6H, non-cubic phase) and β-type phase (3C, cubic phase) are most frequently used for industrial purposes. In particular, 4H SiC is applied more to power device applications that require high voltage, power and frequency as it has a higher bandgap, breakdown voltage and carrier mobility than those of other SiC polytypes [1–4].

There are different methods to grow single crystal SiC, but the physical vapor transport (PVT) method is the most useful as it has the advantages of yielding a large diameter and high growth rate. The most important factor in growing single crystal SiC is to contain and reduce the occurrence of defects (micropipe, pour, polytype) and dislocations (screw, edge, basal plane). Causes for defects and dislocations during the growth process of single crystal SiC include damage, contamination on the seed surface and stress from the temperature gradient of the seed. Additional elements include polytype, particle size, Si/C ratio and impurity of the SiC powder source. The vapor phase composition changes during the SiC growth process according to the metallic atom ion of SiC, $SiO_2$ impurities, and excess Si and C. Micropipes and various dislocations are caused from changes in the stacking arrangement and pressure. If the grain size of the powder decreases, agglomeration easily occurs during sublimation. Increased Si oxide on the surface leads to an increase in the unreacted Si and Si/C ratio, which both cause defects such as misfit dislocation and stacking faults [5–9].

β-phase SiC powder instead of α phase SiC, powder was used to reduce the defect factors and grow high quality single crystal

*Corresponding author. Tel.: +82 2 2123 2852; fax: +82 2 312 5375.
*E-mail address:* drchoidj@yonsei.ac.kr (D.J. Choi).

0272-8842/$ - see front matter © 2013 Elsevier Ltd and Techna Group S.r.l. All rights reserved.
http://dx.doi.org/10.1016/j.ceramint.2013.08.041

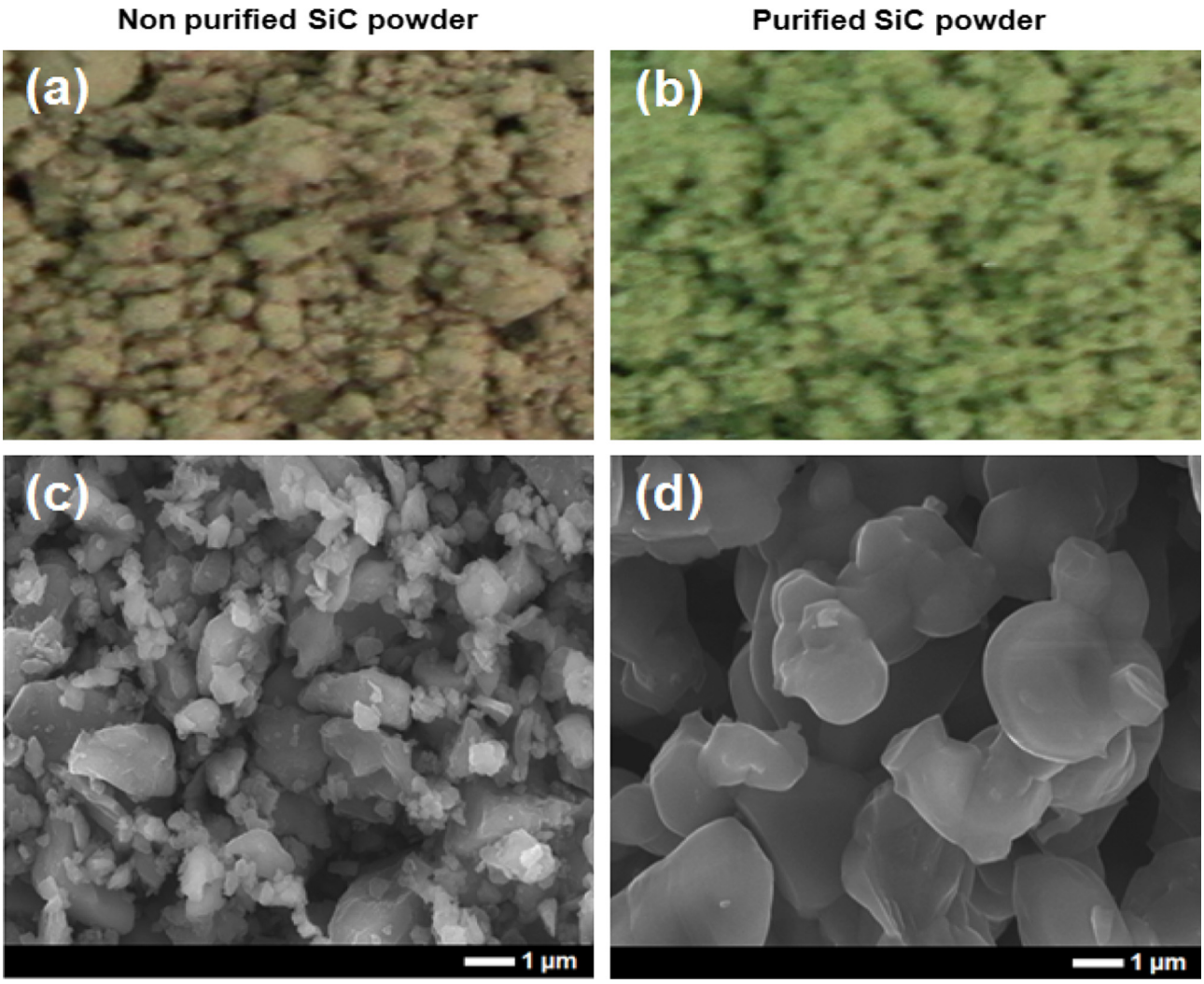


Fig. 1. Optical photograph of (a) non-purified and (b) purified β-SiC powder. Field emission scanning electron microscopy images of (c) non-purified and (d) purified SiC powder with different structures and particle sizes. (For interpretation of the references to color in this figure the reader is referred to the web version of this article.)

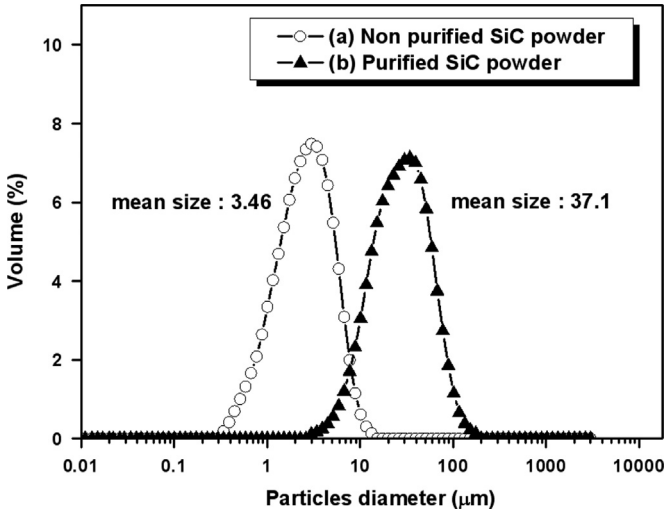


Fig. 2. Particle size distribution analysis results of (a) non-purified and (b) purified SiC powder.

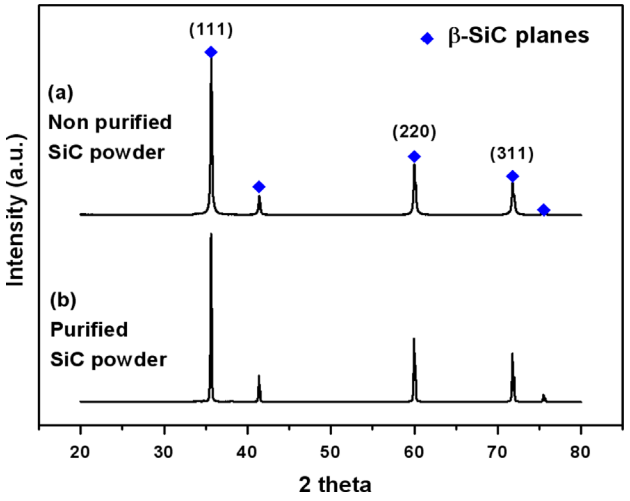


Fig. 3. X-ray diffraction spectra of (a) non-purified and (b) purified SiC powder.

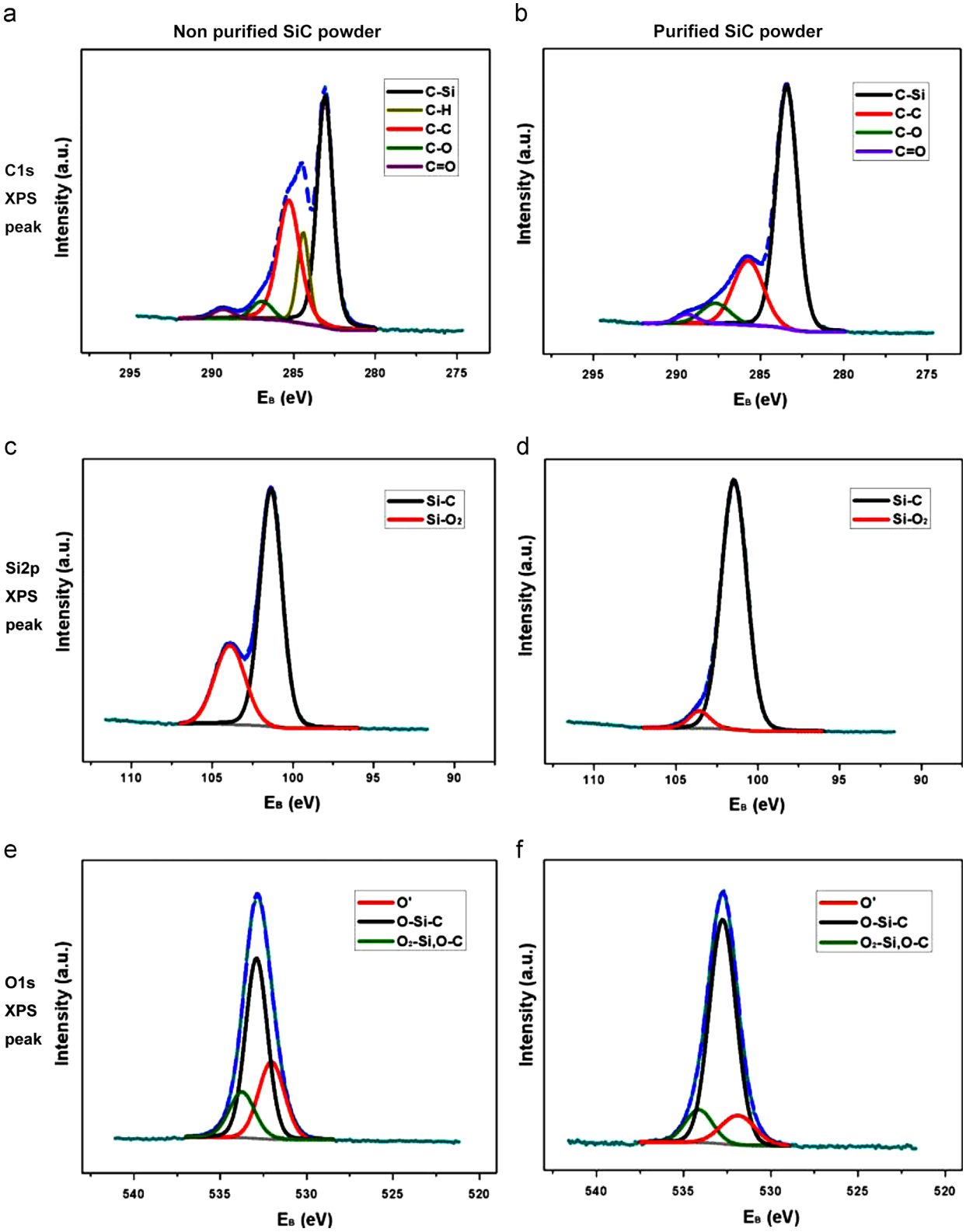


Fig. 4. Chemical state of the β-SiC powder analyzed by XPS: C1s XPS spectra of (a) non-purified and (b) purified SiC powder, S2p XPS spectra of (c) non-purified and (d) purified SiC powder, and O1s XPS spectra of (e) non-purified and (f) purified SiC powder.

4H SiC as it has a high melting point. The aim was to reduce the temperature gradient between the source and seed and minimize the graphitization of the powder source. Furthermore, a purification process of the β-SiC powder was performed to 1) reduce the powder impurities, 2) improve the purity of SiC by creating a Si/C ratio stoichiometry, 3) reduce agglomeration of the SiC powder during sublimation and 4) produce a uniform grain size that significantly influenced the vapor transport and sublimation

rate of the SiC powder. Single crystals of 4H SiC with purified and non-purified powder were grown for wafers, and the distribution of defects and dislocation density were compared.

## 2. Experimental procedure

β-SiC powder (3.46 μm) was purified and the particle size controlled using a vaporization–condensation method. β-SiC powder (100 g) was transferred to a graphite crucible and heated under Ar ambient to 1850 °C with a 15 °C/min heating rate, and held for 15 min. The temperature was then increased to 2000 °C at 2 °C/min and held again. The sample was cooled to 1850 °C and then heated to 2000 °C. This step was repeated three times, resulting in high purity β-SiC powders.

Using purified and non-purified powders, single crystal 4H SiC was grown by the PVT method at a growth temperature of 1900 °C under Ar ambient and a 250 μm/h growth rate. The grown 4H SiC crystals were sliced approximately perpendicular to the growth direction into (0001) Si wafers.

The microstructure and size of the SiC powders were examined using scanning electron microscopy (SEM, JEOL, JSM-7001F). X-ray powder diffraction analysis was performed using an X-ray diffractometer ($2\theta$ method, Rigaku, D/MAX-2500H) with a Cu target to identify the crystalline phase of the powder. The chemical bonding state of the element before and after purification was analyzed by X-ray photoelectron spectroscopy (XPS, K-alpha, Thermo VG) with monochromatic Al Kα ($h\nu$=1486.6 eV) excitation radiation using a 360 W source power at an 12 kV acceleration voltage. Photoelectrons from the Si2p, C1s, and O1s core levels were recorded using a hemispherical analyzer with a 50 eV pass energy and 0.1 eV step size. To analyze the content of the metal ions within the single crystal 4H SiC wafer, time of flight secondary ion mass spectrometry (TOF-SIMS, ion TOF, TOF-SIMS-5) was performed with a $Cs^+$ primary ion source, respectively. Micropipe density and dislocation density distribution maps were analyzed using an automated optical microscopy system.

## 3. Results and discussion

### 3.1. Microstructure and grain size of the β-SiC powder

To produce a high-quality ceramic-using powder, the particle should have a small size with a narrow range and be agglomeration-free with a spherical shape and high purity [10]. In the case of the SiC powder source using the sublimation method, if the particle size is small, agglomeration can easily occur and the packing density decreases due to the large specific surface area and high surface energy [11]. Therefore, the powder was purified to meet the conditions explained, excluding particle size.

Fig. 1 shows the optical photographs (a, b) and SEM images (c, d) of purified and non-purified SiC powder. Non-purified SiC powder was dark gray whereas it turned green after purification. Contamination from impurities on the SiC surface potentially affected the gray color, which changed during the purification process as the impurities decreased. As shown in the SEM images, the non-purified SiC powder shows irregular particle size and structure, and a plate-like shape of the partially sintered β-SiC, while the purified β-SiC powder had a uniformly spherical structure and larger particle size. More metallic ions and SiO$x$ occurred when the particle size of the powder was smaller [12,13]. Therefore, the impurities decreased as the particle size of the powder increased during the purification process. A detailed analysis on this phenomenon was performed via investigation of the chemical composition.

Fig. 2 is the analysis of the particle size distribution of β-SiC powder before and after purification. The average particle size of non-purified powder was 3.46 μm which increased to 37.1 μm after purification. The particle coarsened from surface and bulk diffusion due to thermal reduction during the purification process [14]. XRD analysis was used to investigate whether the polycrystalline particle occurred partially or wholly during the process (Fig. 3). Both purified and non-purified powder clearly showed major peaks at the (111), (220) and (311) planes, indicating β-SiC without other elements. Therefore the purification condition was appropriate as crystallographic transformation of β-SiC did not occur.

Table 1
Photoelectron binding energies and content percentages of non-purified and purified SiC powder.

| **Non-purified SiC powder** | | | | **Purified SiC powder** | | | |
|---|---|---|---|---|---|---|---|
| Composition spin | Bond | Binding energy (eV) | Content percentage | Composition spin | Bond | Binding energy (eV) | Content percentage |
| C1s | C–Si | 283.0 | 46.73 | C1s | C–Si | 283.4 | 80.94 |
| | C–H | 284.4 | 12.84 | | | | |
| | C–C | 285.2 | 28.59 | | C–C | 285.6 | 19.16 |
| | C–O | 286.9 | 8.64 | | C–O | 287.3 | 3.54 |
| | C=O | 289.3 | 3.21 | | C=O | 289.7 | 2.54 |
| Si2p | Si–C | 101.3 | 68.63 | Si2p | Si–C | 101.4 | 92.06 |
| | $Si–O_2$ | 103.9 | 31.37 | | $Si–O_2$ | 103.5 | 7.94 |
| O1s | O′ | 531.6 | 10.47 | O1s | O′ | 531.5 | 2.33 |
| | O–Si–C | 532.8 | 83.96 | | O–Si–C | 532.7 | 94.88 |
| | $O_2$–Si | 533.5 | 5.57 | | $O_2$–Si | 533.4 | 2.89 |

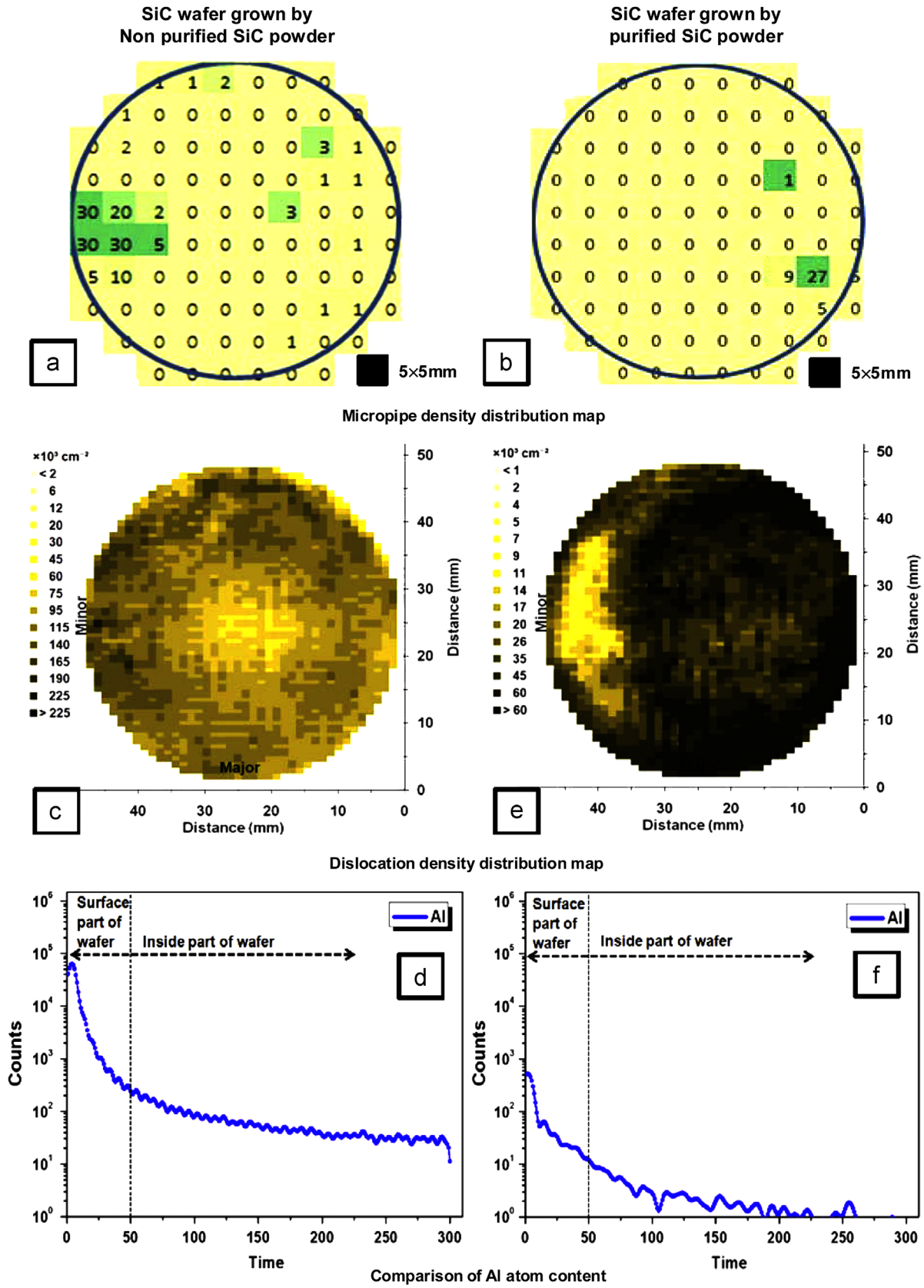


Fig. 5. Comparison of the micropipe and dislocation density distribution map between 4H SiC wafers grown by (a, c) non-purified and (b, d) purified SiC powder. TOF-SIMS measurements of the Al atom content within the 4H SiC wafer grown with non-purified and purified powder (e, f).

### 3.2. Chemical component analysis of the β-SiC powder

During the growth process of the SiC powder, vapor phases occurring from sublimation of the SiC powder are Si, SiC, $Si_2C$, and $SiC_2$ [15]. However, the grain of the SiC powder source is covered with free carbon, an oxide phase such as silica ($SiO_X$) and silicon oxycarbide ($SiC_xO_y$). When the powder was high in $SiO_2$, more reactive gaseous species appeared. $SiO_2$ reacts with metallic ion impurities, which causes changes in the vapor phase composition leading to defects [12,16]. Fig. 4 is an analysis of the powder chemical component before and after purification by narrow scanning of the XPS peaks of C1s, Si2p, and O1s. The C1s XPS spectra of the non-purified powder in Fig. 4(a) show C–H, C–O and C–C that have high bonding energy, and C–Si bonding at the binding energy 283 eV position. The hydrocarbon species peak, which was not observed in Fig. 4(b) of the purified SiC powder, was due to the contaminated carbon and oxygen. Additionally, permeated hydrogen can become hydride by reacting with carbon and can affect SiC bonding through the $H_2$ reaction with carbon due to its high chemical activity [17]. The analysis results of the Si2p spectra in Fig. 4(c) and (d) confirmed that the purified and non-purified powders had a Si–C binding energy of 101.36 eV. The non-purified powder showed the Si–$O_2$ spectra moving towards a high binding energy due to the high oxygen content. The Si–$O_2$ content was high and the Si–C bonding was low as the high oxygen content broke Si–C bonding, and oxygen atoms entered into a more stable carbon site to become $SiO_2$ [18]. As shown in Table 1, purified SiC powder had less Si–$O_2$ and the Si–C bonding increased to more than 90%. Fig. 4(e) and (f) compares the O1s spectra between purified and non-purified SiC powder. O–Si–C has a binding energy of 532.8 eV. O′ (531 eV) indicates a C–O–C and the Si–O–Si bridge or Si–O–C was observed with $O_2$–Si or O–C bonding that had a 533 eV binding energy. O′ is an amorphous metastable phase where the O atom enters the Si back bond, and the silicon atom bonds the oxygen and carbon atoms. As the dangling bond of the Si atom changes when O′ species are observed, more defects are present [19,20]. Additionally, non-purified powder has more defects as it has more O′ content than purified powder.

As a result of analyzing the chemical component of the SiC powder before and after purification with XPS, the purity and content of SiC were confirmed to increase during the purification process as impurities such as SiO*x*, carbon and silicon oxycarbide can cause various defects to decrease.

### 3.3. Mapping of micropipes and dislocations in the 4H SiC wafer

Fig. 5 is a comparison of automatically measured micropipes and the dislocation density of 2-in. single crystal 4H SiC wafers grown with purified and non-purified SiC powder. A single crystal 4H SiC wafer grown with SiC powder before purification showed a 6 $cm^{-2}$ micropipe density and 9.7$E^{+4}$ $cm^{-2}$ dislocation density. However, the single crystal 4H SiC wafer grown with purified powder showed a 2.1 $cm^{-2}$ micropipe density and 4.7$E^{+4}$ $cm^{-2}$ dislocation density, demonstrating better quality than that of the single crystal 4H SiC wafer grown with non-purified powder. This occurred when identical factors were used that affect the growth of the crystal such as the growth temperature, pressure and distance between the source and seed with varied SiC source powder, through which we confirmed that the growth of the micropipes and dislocations reduced when the purified powder was used.

Fig. 5(e) and (f) compares the metallic ion Al content in wafers measured by TOF-SIMS. The Al content in the single crystal 4H SiC wafer grown by purified powder was much lower. The Al atom within the powder is similar in the size to the Si atom when sublimated, and it intrudes on the space of the Si to produce a lattice dislocation [21]. Al also causes a void and vacancy leading to defects during stacking. Although these direct factors affect the results, there are likely more composite factors in reduced micropipe and dislocation density when using the purified powder. First, although β-SiC powder with a higher Si/C ratio than that of α-SiC powder was used, excess carbon and silicon causing micropipes were reduced by the increased SiC content through the purification process. Second, by using β-SiC powder that has a low melting point, thermal stress occurring between the seed and source decreased. Third, the particle size of the powder increased through the purification process to reduce the metallic ions and SiO in the surface, increase the packing density and decrease graphitization of the powder surface. Fourth, $SiO_2$ was reduced from purification to diminish the reaction of the metallic ions, which led to less change in the vapor phase composition and more stable Si partial pressure. Lastly, various impurities within the powder were reduced from purification so that parasitic nucleation within the seed and growth interface decreased.

## 4. Conclusion

β-SiC powder was purified and the particle size controlled using a vaporization–condensation method. After vaporization–condensation from 2000 to 1850 °C, the small particle size of β-SiC powder increased to an average particle size (greater than 37 μm) and the formerly irregular structure took a regular spherical shape with purity. The phase translation of β-SiC did not occur during the thermal process while being purified. Purified β-SiC powder showed decreased metallic and $SiO_2$ impurities that can affect temperature, pressure and vapor phase composition during SiC crystal growth and demonstrated increased SiC content compared to non-purified powder. The micropipe and dislocation density of the single crystal 4H SiC grown by purified β-SiC powder were reduced by 3.9 $cm^{-2}$ and 5 $E^{+4}$ $cm^{-2}$, respectively, compared to the single crystal 4H SiC grown by a non-purified powder. In conclusion, the quality of the 4H SiC wafer improved through purification of the β-SiC powder.

## Acknowledgment

This research was conducted with support from the International Collaborative Research and Development Program of the Korea Institute for the Advancement of Technology.

## References


[1] J.C. Zolper, M. Skowronski, Advances in silicon carbide electronics, Materials Research Society Bulletin 30 (2005) 273–278.

[2] H. Morkoc, S. Strite, G.B. Gao, M.E. Lin, B. Sverdlov, M. Burnes, Large-band-gap SiC, III–V nitride, and II–VI ZnSe-based semiconductor device technologies, Journal of Applied Physics 76 (1994) 1363–1396.

[3] D. Nakamura, I. Gunjishima, S. Yamaguchi, T. Ito, A. Okamoto, H. Kondo, S. Onda, K. Takatori, Ultrahigh-quality silicon carbide single crystals, Nature 430 (2004) 1009–1012.

[4] W.Y. Ching, Y.N. Xu, P. Rulis, L. Ouyang, The electronic structure and spectroscopic properties of 3C, 2H, 4H, 6H, 15R and 21R polymorphs of SiC, Materials Science and Engineering A 422 (2006) 147–156.

[5] M. Kanaya, J. Takahashi, Y. Fujiwara, A. Moritani, Controlled sublimation growth of single crystalline 4H-SiC and 6H-SiC and identification of polytypes by x-ray diffraction, Applied Physics Letters 58 (1991) 56–59.

[6] Yu.M. Tairov, V.F. Tsvetkov, Progress in controlling the growth of polytypic crystals, Progress in Crystal Growth and Characterization of Materials 7 (1983) 111–162.

[7] D. Schulz, G. Wagner, J. Dolle, K. Irmscher, T. Muller, H.J. Rost, D. Siche, J. Wollweber, Impurity incorporation during sublimation growth of 6H bulk SiC, Journal of Crystal Growth 198 (1999) 1024–1027.

[8] M. Anikin, R. Madar, Temperature gradient controlled SiC crystal growth, Materials Science and Engineering B 46 (1997) 278–286.

[9] R. Ma, H. Zhang, V. Prasad, M. Dudley, Growth kinetics and thermal stress in the sublimation growth of silicon carbide, Crystal Growth and Design 2 (2002) 213–220.

[10] J.H. Flint, J.S. Haggerty, Ceramic powders from laser driven reations, SPIE Application of Lasers to Industrial Chemistry 458 (1984) 108–113.

[11] W. Gang, M. Yuedong, Z. Shaofeng, L. Feng, J. Zhongqing, S. Xingsheng, R. Zhaoxing, W. Xiangke, Surface modification of nanometre silicon carbide powder with polystyrene by Inductively Coupled Plasma, Plasma Science and Technology 10 (2008) 79–82.

[12] H. Tanaka, H.N. Yoshimura, S. Otani, Y. Zhou, M. Toriyama, Influence of silica and aluminum contents on sintering of and grain growth in 6H-SiC powders, Journal of the American Ceramic Society 83 (2000) 226–228.

[13] S.Y. Chong, H.V. Atkinson, H. Jone, Effect of ceramic particle size, melt superheat, impurities and alloy additions on threshold pressure for infiltration of SiC powder compacts by aluminium-based melts, Materials Science and Engineering A 73 (1993) 233–237.

[14] V.M. Kevorkijan, M. Komac, D. Kolar, Low-temperature synthesis of sinterable SiC powders by carbothermic reduction of colloidal $SiO_2$, Journal of Materials Science 27 (1992) 2705–2712.

[15] Q.S. Chen, H. Zhang, R.H. Ma, V. Prasad, C.M. Balkas, N.K. Yushin, Modeling of transport processes and kinetics of silicon carbide bulk growth, Journal of Crystal Growth 225 (2001) 299–306.

[16] K. Shimoda, J.S. Park, T. Hinoki, A. Kohyama, Influence of surface structure of SiC nano-sized powder analyzed by X-ray photoelectron spectroscopy on basic powder characteristics, Applied Surface Science 253 (2007) 9450–9456.

[17] N.K. Huang, D.Z. Wang, Q. Xiong, B. Yang, XPS study of hydrogen permeation effect on SiC–C films, Nuclear Instruments and Methods in Physics Research Section B 207 (2003) 395–401.

[18] M. Sreemany, T.B. Ghosh, B.C. Pai, M. Chakraborty, XPS studies on the oxidation behavior of SiC particles, Materials Research Bulletin 33 (1998) 189–198.

[19] C. Onneby, C.G. Pantano, Silicon oxycarbide formation on SiC surfaces and at thr $SiC/SiO_2$ interface, Journal of Vacuum Science and Technology A 15 (1997) 1597–1602.

[20] Y. Hijikata, H. Yaguchi, M. Yoshikawa, S. Yoshida, Composition analysis of $SiO_2$/SiC interfaces by electron spectroscopic measurements using slope-shaped oxide films, Applied Surface Science 184 (2001) 161–166.

[21] F. Bernardini, L. Colombo, Interaction of doping impurities with the 30 partial dislocations in SiC: an ab initio investigation, Physical Review B 72 (2005) 0852151–08521510.